Asian Journal of Physics Vol. 24, No 2 (2015) 335-344

Optical processing for radar imaging and broadband signal

Francis T S Yu
Emeritus Evan Pugh Professor of electrical Engineering Penn State University
University Park, PA 16802, USA

One of the interesting applications in optical processing must be the synthetic aperture radar imaging. It was the first time that a naked human eye can actually see the radar image with optics. By exploiting the optical two-dimensional spatial processing capability, we will show that a very large space bandwidth signal can be processed by means of conventional optical information processor.

1 Synthetic-Aperture Radar Imaging

One of the interesting applications of optical processing must be to the synthetic-aperture antenna data or side-looking antenna imaging. Let us consider a side-looking radar system carried by an aircraft in level light shown in Fig 1, in which we assume a sequence of pulsed radar signals is directed at the terrain and the return signals along the flight path are received. Let the cross-track coordinate of the radar image as ground range coordinate and the along-track coordinate as azimuth coordinate, then the coordinate joining the radar trajectory of the plane of any target under consideration as can be defined as slant range as shown in Fig 2. In the words the azimuth resolution will be in the order of $\lambda\, r_1/D$, where λ is the wavelength of the radar signals, r_1, is the slant range, and D is the along-track dimension of the antenna aperture. Since the radar wavelength is several orders of magnitude larger than the optical wavelength, a very large antenna

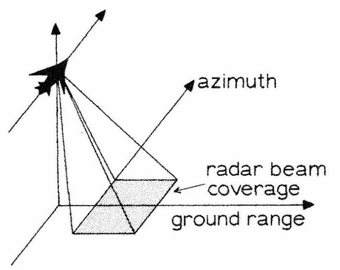

Fig 1. Side-looking Radar

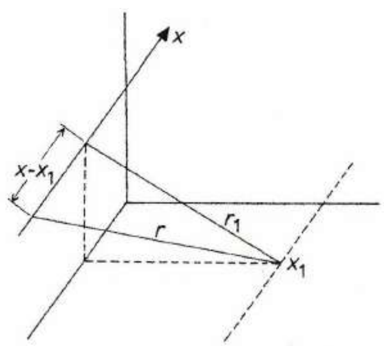

Fig 2. Geometry of side-looking radar

aperture D is required to have an angular resolution comparable to that of a photo reconnaissance system.

Corresponding author :
e-mail: ftyece@engr.psu.edu (Francis T S Yu)

The required antenna length may be hundreds, or even thousands of feet and it is impractical to realize on an aircraft. Nevertheless this difficulty can be resolved by means of the synthetic-aperture technique, as will be shown in the following:

Let us assume that the aircraft carries a small side-looking antenna and a relatively broad beam radar signal is used to scan the terrain, by virtue of the aircraft motion. The radar pulses are emitted in a sequence of positions along the flight path, which can be treated as if they were the positions occupied by the elements of a linear antenna array. The return radar signal at each of the respective positions can be recorded coherently as a function of time with a local reference signal for which the amplitude and the phase quantities are simultaneously encoded. The complex waveforms are then properly combined to simulate a long-aperture element-antenna!

For simplicity, we consider first a point-target problem and then can be quickly extended to multi-target situation owning to spatial invariance condition. Since the radar signal is produced by periodic rectangular pulses modulated with a sinusoidal signal, the pulse periodic gives the range information and the azimuth resolution is provided by the distance traveled by the aircraft between pulses, which is smaller than $\pi/\Delta p$, where Δp is the spatial bandwidth of the terrain reflections. Thus the returned radar signal can be written as

$$S_1(t) = A_1(x_1, r_1)\ \exp\left\{i\left[\omega t - 2kr_1 - \frac{k}{r_1}(x - x_1)^2\right]\right\} \tag{1}$$

where A_1 is an appropriate complex constant.

Now if we consider the terrain at range r_1 consists of a collection of N points targets, then by superposing the returned radar signals we have,

$$S(t) = \sum_{n=1}^{N} S_n(t)$$

$$= \sum_{n=1}^{N} A_n(x_n, r_1)\ \exp\left\{i\ \left[\omega t - 2kr_1 - \frac{k}{r_1}(v\ \ t - x_n)^2\right]\right\} \tag{2}$$

where v is the velocity of the aircraft. If the returned radar signal is synchronously demodulated, the demodulated signal can be written as,

$$S(t) = \sum_{n=1}^{N} \left|A_n(x_n, r_1)\right|\ \cos\ \left[\omega_c\, t - 2kr_1 - \frac{k}{r_1}(v\ \ t - x_n)^2 + \phi_n\right] \tag{3}$$

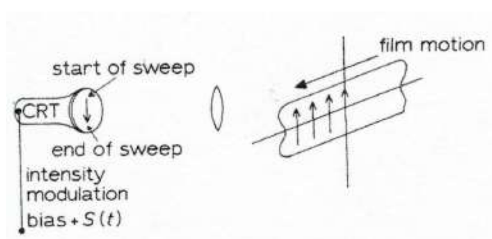

Fig 3. Recording of the returned radar signal for subsequent optical processing

where ω_c is the arbitrary carrier frequency and ϕ_n is the arbitrary phase angle. In order to display the return radar signal of Eq (3) on a cathode-ray tube, the demodulated signal is used to modulate the intensity of the electron beam, which is swept vertically across the cathode-ray tube in synchronism with return radar pulses (Fig 3). If this modulated cathode-ray display is imaged on a strip of photographic film, which is drawn at a constant horizontal velocity, then the successive range traces will be recorded side by side, producing a two-dimensional format (Fig 4).

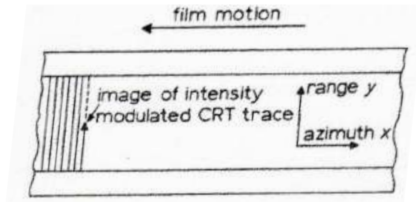

Fig 4. Radar signal recording format.

The vertical lines represent the successive range sweeps and the horizontal dimension represents the azimuth position, which is the sample version of $s(t)$. This sampling is carried out in such a way that, by the time the samples have been recorded on the film, it is essentially indistinguishable from the un-sampled version. In this recording, in which the time variable is converted to a space variable as defined in terms of distance along the recorded film. With the proper reading exposure, the transparency of the recorded film represents the azimuth history of the returned radar signals. Thus, considering only the data recorded along the line y-y1, on the film, the transmittance can be written as

$$T(x_1, y_1) = K_1 + K_2 \sum_{n=1}^{N} \left| A_n(x_n, r_1) \right| \cos\left[\omega_x x - 2kr_1 - \frac{k}{r_1}\left(\frac{v}{v_f} x - x_n\right)^2 + \phi_n \right] \tag{4}$$

where K_s are bias constants and $x = v_f t$, v_f is the speed of film motion, and $\omega_f = \omega_c / v_f$

For simplicity in illustration, we restrict ourself to single target problem (i.e., $n = 1$); for which the first exponential term of the cosine function in Eq (4) can be written as

$$T_1(x_1, y_1) = C \exp(i\ \omega_x\ x) \exp\left[-i \frac{k}{r_1}\left(\frac{v}{v_f}\right)^2 \left(x - \frac{v_f}{v} x_j\right)^2 \right] \tag{5}$$

In which we see that it is essentially a one-dimensional Fresnel lens (or 1D hologram) equation. The first linear phase factor ($\omega_x x$) represents a prism with an oblique angle of

$$\sin\theta = \frac{\omega_x}{k_1} \tag{6}$$

where $k_1 = 2\pi/\lambda_1$ with λ_1 wavelength of the illuminating light source. And the second term represents a cylindrical lens centered at

$$x = \frac{v_f}{v} x_j \tag{7}$$

With a focal length of

$$f = \frac{1}{2} \frac{\lambda}{\lambda_1} \left(\frac{v_f}{v} \right)^2 r_1 \tag{8}$$

Needless to say that for N targets, the corresponding cylindrical lenses would be centered at

$$x = \frac{v_f}{v} x_n, \quad n = 1,\ 2, \cdots, N \tag{9}$$

In order to reconstruct the radar imagery, the scanned radar transparency is illuminating by a monochromatic plane wave, as depicted in Fig 5 in which we show that the real and virtual images can be reconstructed relative to the positions of the point images along the foci of the lens-like structure of the recorded transparency, which are determined by the positions of the point targets.

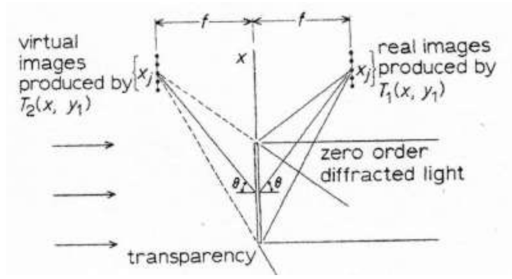

Fig 5. Image reconstruction produced by the film transparency.

However, the reconstructed images will be spread in the y direction; this is because the transparency is realizing a one-dimensional function along $y = y_i$, and hence exerts no focal power in this direction.

Since it is our aim to reconstruct an image not only in the azimuth direction but also in the range direction, it is necessary to image the y coordinate directly onto the focal plane of the azimuth image. Thus to construct the terrain map, we must image the y coordinate of the transmitted signal onto a tilted plane determined by the focal distances of the azimuth direction. This imaging procedure can be carried out by inserting a positive conical lens immediately behind the scanned radar image transparency shown in Fig 6.

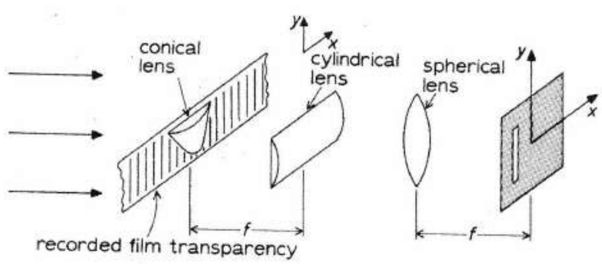

Fig 6. An optical processing system for imaging synthetic-antenna data.

It is clear that if the transmittance of the conical lens is given by

$$T_1(x_1, y_1) = \exp\left(-i\frac{k_1}{2f}x^2\right) \tag{10}$$

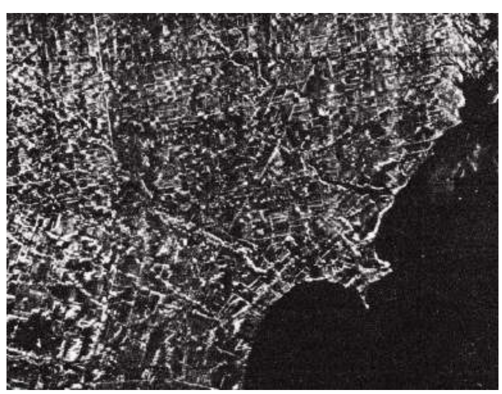

Fig 7. Synthetic-aperture radar image of the Monroe, Michigan area, (Permission by L.J. Cutrona)

then it is possible to remove the entire tilted plane of all the virtual diffraction to the point at infinity, while leaving the transmittance in the y direction unchanged. Thus if the cylindrical lens is placed at the focal distance from the scanned radar transparency, it will create a virtual image of the y direction at infinity. Now the azimuth and the range images (i.e., x and y direction) are at the point of infinity for which can be brought back to a finite distance with a spherical lens. Thus we see that radar imagery can be constructed at the output plane, through a slit, of the optical processing system. An example of the radar imagery is shown in Fig 7, in which we see a variety of scatters, including city streets, wooded areas, and farmlands. Lake Erie, with some ice floes, can be seen on the right.

2 Optical Processing of Broadband Signals

Another interesting application of optical processing is to broadband signals analysis. One of the basic limitations of the multichannel optical analyzer is that the resolution is limited by the width of the input aperture and this limitation can be alleviated by using a two-dimensional raster scan input transparency shown in Fig 8.

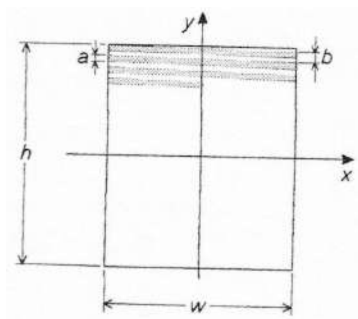

Fig 8. Raster scan input signal transparency

Thus we see that if scanned format transparency is presented to input plane of an optical processor, then the complex light distributed at the output plane would be the Fourier transform of the input scanned format. Thus a large space-bandwidth signal analysis can be obtained with the scanned format.

Let us assume that a broadband signal is raster scanned on a spatial light modulator (or on a strip of transparency), in which we assumed that the scan rate has been adjusted to accommodate the maximum frequency content of the broadband signal, as represented by

$$v \geq \frac{f_m}{R} \tag{11}$$

where v is the scan velocity, f_m is the maximum frequency content of the broad band signal, and R is the resolution limit of the optical system.

If this format is presented at the input plane of the optical analyzer, then the complex light field distributed at the output plane can be shown by

$$F(p,q) = C_1 \sum_{n=1}^{N} \operatorname{sinc}\left(\frac{qa}{2}\right) \left\{ \operatorname{sinc}\left(\frac{pw}{2}\right) * F(p) \ \ \exp\left[i\frac{pw}{2}(2n-1) \right] \right\} \times \exp\left\{ -i\frac{q}{2}\left[h - 2(n-1)b - a \right] \right\} \tag{12}$$

where C_1 is a complex constant, and

$$F(p) = \int f(x')\exp(-i\,p\,x')dx'$$

$$x' = x + (2n-1)\frac{w}{2}, \text{ and } \operatorname{sinc} X \overset{\Delta}{=} \frac{\sin X}{X} \tag{13}$$

For simplicity, let us assume that the broadband signal is a simple sinusoid i.e.,

$$f(x') = \sin p_0 x' \tag{14}$$

then we have

$$F(p,q) = C_1 \operatorname{sinc}\left(\frac{qa}{2}\right) \sum_{n=1}^{N} \left\{ \operatorname{sinc}\left(\frac{pw}{2}\right) * \frac{1}{2}\left[\delta(p-p_0)+\delta(p+p_0)\right] \times \exp\left[i\frac{w\,p_0}{2}(2n-1)\right]\right\} \exp\left\{-i\frac{q}{2}\left[w-2(n-1)b\right]\right\} \tag{15}$$

To further simplify the analysis, we consider only one of the components, we have

$$F_1(p,q) = C_1 \operatorname{sinc}\left[\frac{w}{2}(p-p_0)\right] \ \operatorname{sinc}\left(\frac{qa}{2}\right) \ \exp\left(-i\frac{qw}{2}\right) \ \times \sum_{n=1}^{N} \exp\left[i\frac{1}{2}(2n-1)(wp_0+bq)\right] \tag{16}$$

The corresponding intensity distribution is given by

$$I_1(p,q) = \left|F_1(p,q)\right|^2 = C_1^2 \operatorname{sinc}^2\left[\frac{w}{2}(p-p_0)\right] \ \operatorname{sinc}^2\left(\frac{qa}{2}\right) \ \times \sum_{n=1}^{N} \exp\left[i2n\theta\right] \sum_{n=1}^{N} \exp\left[-i2n\theta\right] \tag{17}$$

where

$$\theta = \frac{1}{2}(w\,p_0 + b\,q) \tag{18}$$

But

$$\sum_{n=1}^{N} e^{i2n\theta} \ \sum_{n=1}^{N} e^{-i2n\theta} = \left(\frac{\sin N\theta}{\sin\theta}\right)^2 \tag{19}$$

thus we have

$$I_1(p,q) = C_1^2 \operatorname{sinc}^2\left[\frac{w}{2}(p-p_0)\right] \cdot \operatorname{sinc}^2\left(\frac{qa}{2}\right) \cdot \left(\frac{\sin N\theta}{\sin\theta}\right)^2 \tag{20}$$

In view of this equation, we see that that the first sinc factor represents a relatively narrow spectral line in the p direction, located at $p = p_0$, which is derived from the Fourier transform of a pure sinusoid truncated within the width of the input transparency. The second sinc factor represents a relatively broad spectral band in the q direction, which is derived from the Fourier transform of a rectangular pulse of width (i.e., the channel width). And the last factor deserves special mention for large N (i.e., scanned lines), the factor approaches a sequence of narrow purses located at

$$q = \frac{1}{b}(2\pi\, n - w\,p_0)\,, \quad n = 1, 2, \dots \tag{21}$$

Notice that this factor yields the fine spectral resolution in the q direction.

Let us confine within a relatively narrow region in p direction that is the half-width of the spectral spread as given by

$$\Delta p = \frac{2\pi}{w} \tag{22}$$

which is the resolution limit of an ideal transform lens. In the q direction, the irradiance is first confined within a relatively broad spectral band, (primarily depends on the channel width) centered at $q = 0$, and it is modulated by a sequence of narrow periodic pulses. The half-width of the broad spectral band is given by

$$\Delta q = \frac{2\pi}{a} \tag{23}$$

The separation of the narrow pulses is obtained from a similar equation,

$$\Delta q_1 = \frac{2\pi}{b} \tag{24}$$

It may be seen from the preceding equation, there will be only a few pulses located within the spread of the broad spectral band for each p_0, as shown in Fig 9.

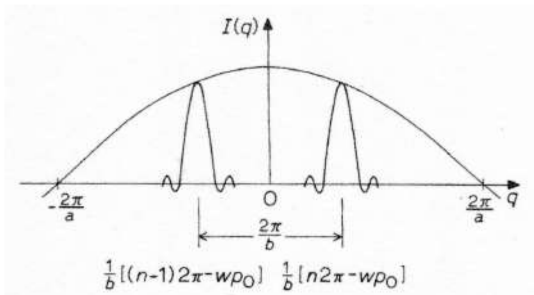

Fig 9. A broad spectral band modulated by a sequence of narrow pulses.

Notice that, the actual location of any of the pulses is determined by the signal frequency. Thus, if the signal frequency changes, the position of the pulses also changes, in accordance with

$$dq = \frac{w}{b} dp_0 \tag{25}$$

We further note that the displacement in the q direction is proportional to the displacement in the p direction. The output spectrum includes the required frequency discrimination, which is equivalent to analysis of the entire signal in one continuous channel. In order to avoid the ambiguity in reading the output plane, all but one of the periodic pulses should be ignored. This may be accomplished by masking the entire output plane except the region, shown in Fig 10. Thus we see that, as the input signal frequency advances one pulse leaves the open region and another pulse enters the region. As a result a single bright spot would be scanned out diagonally on the output plane. The frequency locus of the input signal can be determined in cycles per second. To remove the non-uniformity of the second sinc factor, a weighting transparency may be placed at the output plane of the processor.

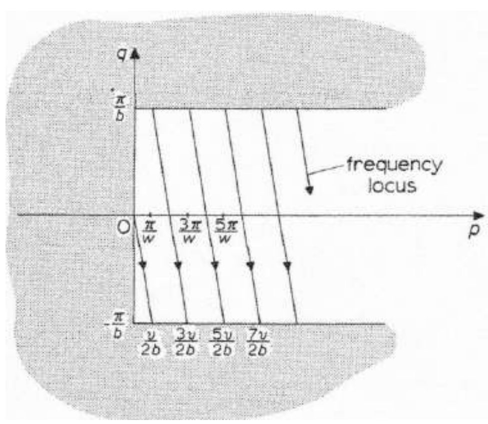

Fig 10. Frequency loci at the output spectral plane.

Although our analysis was carried out on a one-frame basis, the operation can be performed on a continuously running manner, as the input scanned raster format is continuously moving in q direction.

3 Broad-Band signal Processing with Area Modulation

Area maculation for movie sound track recording had been used in years. And the formats can also be used for spectrum analysis. There are however two formats have been used, namely the unilateral and bilateral shown in Fig 11.

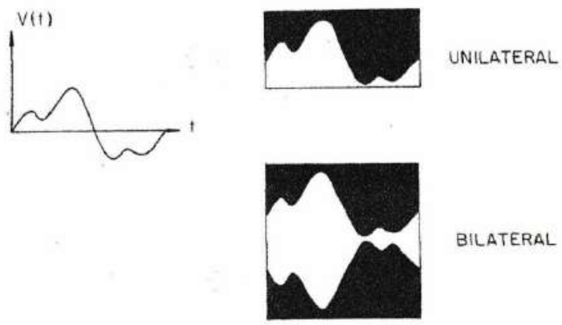

Fig 11. Unilateral and Bilateral area modulation formats.

Notice that area modulation has the advantages of simplicity implementation and the nonlinearity of the density modulation can be avoided, but there is a trade-off for input spatial limited resolution. Let us now describe the area modulation transmittance functions for unilateral and bilateral respectively as follows;

$$T_1(x,y) = rect\left(\frac{x}{L}\right) \quad rect\left\{\frac{y}{2\left[B+f(x)\right]}\right\} \tag{26}$$

and

$$T_2(x,y) = rect\left(\frac{x}{L}\right) \quad rect\left\{\frac{y-[f(x)-B]/2}{\left[B+f(x)\right]}\right\} \tag{27}$$

where L is the width of the transmittance, B is the appropriate bias; $f(x)$ is the input function, and

$$rect\left(\frac{x}{L}\right) \overset{\Delta}{=} \begin{cases} 1, & |x| \le L/2 \\ 0, & otherwise \end{cases} \tag{28}$$

If an area modulated transmittance is presented to an optical processor, the correspondent output light distributions can respectively be shown as

$$\begin{aligned} G_1(p,\ 0) &= 2C \int rect\left(\frac{x}{L}\right)\left[B+f(x)\right] \ \exp(-ipx) \ dx \\ &= 2C \int_{-L/2}^{L/2} B \ \exp(-ipx) \ dx \ + \ 2C \int_{-L/2}^{L/2} f(x) \ \exp(-ipx) \ dx \end{aligned} \tag{29}$$

And

$$\begin{aligned} G_2(p,\ 0) &= \int T_2(x,y)\exp(-ipx) \ dx \\ &= C\left[\int_{-L/2}^{L/2} B \ \exp(-ipx) \ dx \ + \int_{-L/2}^{L/2} f(x) \ \exp(-ipx) \ dx\right] = \frac{1}{2}G_1(p,\ 0) \end{aligned} \tag{30}$$

It is now evident that, if is a bilateral sinusoidal area function is implemented as given by

$$f(x) = A \ \sin(p_0 x + \theta) \tag{31}$$

Then the output light distribution can be shown as

$$G_1(p,\ 0) = K1\ \ \delta(p) + K_2\ \ \delta(p - p_0) + K_3\ \ \delta(p + p_0) \tag{32}$$

in which we see that two spectral points located at $p = p_0$ and $p = -p_0$ can be found. In view of this technique, a larger class of recording material can be used, since the recording has the advantage of not restricting to the linear region of the input devise. To sum up this section we provide a section of a speech spectrogram generated by the area modulation technique, shown in Fig 12.

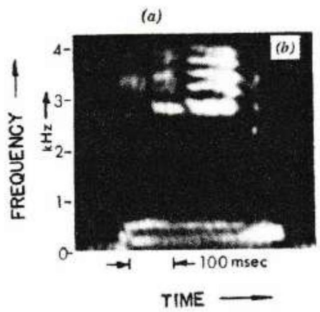

Fig 12. Speech spectrogram obtained by optical processing with area modulation (Courtesy of C C Aleksoff).

Needless to say that, the area modulation technique can also be applied to broad-band spectrum analysis, using the raster scanned format, as shown in Fig 13.

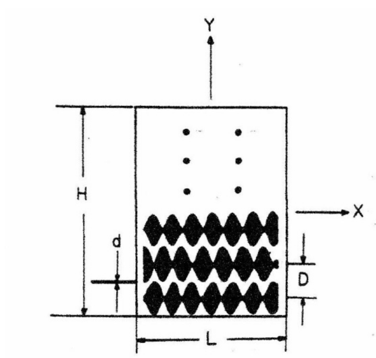

Fig 13. Geometry of area modulated input for wide-band processing.

The corresponding input transmittance to the optical processor can be written as

$$f(x, y) = \sum_{n=1}^{N} rect\left(\frac{x}{L}\right)\ \ rect\left\{\frac{y - n\ \ D}{2\left[B + f_n(x)\right]}\right\} \tag{33}$$

where N is the number of scanned lines. Then by optically performing the Fourier transformation, the output light distribution is given by

$$F(p,\ q) = \sum_{n=-N}^{n=N} C \int_{-L/2}^{L/2} [B + f_n(x)]\text{sinc}\left\{q\left[B + f_n(x)\right]\right\}\ \exp\left[-i(px - nDq)\right]\ dx \tag{34}$$

If we restrict the observation for a single sinusoid, the corresponding output intensity distribution can be shown as

$$I_1(p,q) = \left[K_1\ \text{sinc}\left(\frac{LP}{2}\right)\right]^2 + K_2\left\{\text{sinc}\left[\frac{L}{2}(p - p_0)\right]\right\}^2\ \cdot\left(\frac{\sin N\theta}{\sin\theta}\right)^2 \tag{35}$$

We see that the result is actually similar to the density modulating case as we have described before.

For large value of N (i.e., scanned lines), the last factor would converges to a sequence of narrow periodic pulses located at

$$q = (1/D)\ (2n\pi - L_{p0});\ n = 1, 2, ... \tag{36}$$

Thus we see that as the input frequency changes the location of the pulses change accordingly as given by

$$d_p = (L/D)dp_0 \tag{37}$$

The displacement in the q direction is proportional to the displacement in the p direction. Since the pulse width decreases as the number of scan lines N increases, the output spectrum would yield a frequency discrimination equivalent to that obtained with a continuous signal of NL long.

We further note that as the input frequency advances, one of the pulses leaves the open aperture at $q = -\pi/D$ and a new pulse enters at $q = \pi/D$ which is resulting in a diagonal frequency locus as shown in Fig 14.

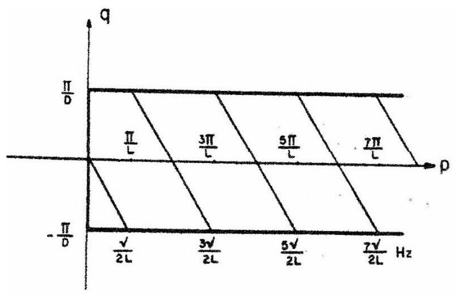

Fig 14. Output spectrum frequency locus.

We emphasize again that area modulation offer the advantage of simple implementation for which the nonlinearity of density modulation can be avoided. However the available space bandwidth product for the processor is smaller. Aside this disadvantage, by efficiently utilize of the two dimensional format, its space bandwidth product is still warrant for many interesting applications.

4 Final remarks

The major advantages of optical information processing must be the massive interconnectivity, very high density, parallel processing capability and others. These are the trademarks for using optical processing. We have shown that synthetic aperture radar imaging can be processed with optics, for which was the first time that naked human eye can actually see radar images, with high resolution. Since optical processing is generally a two-dimensional spatial processor, we have shown by exploiting the two-dimensional processing capability, a very large space-bandwidth signal can actually be processed with a conventional optical processor.

References

1. Cutrona L J, Leith E N, Porcello L J, Vivian W E, On the application of Coherent Optical Processing Techniques to Synthetic-Aperture Radar, *Proc IEEE*, 54(1966)1026.
2. Yu F T S, *Introduction to Diffraction, Information Processing, and Holography*, (MIT Press, Cambridge, Mass.), 1973.
3. Thomas C E, Optical Spectrum Analysis of Large Space-Bandwidth Signals, *Appl Opt*, 5(1966)1782.
4. Tai A, Yu F T S, Wide-Band Spectrum Analysis with Area Modulation, *Appl Opt*, 18(1979)460.
5. Yu F T S, Suganda Jutamulia, Shizhuo Yin, *Introduction to Information Optics*, (Academic Press, San Diego), 2001.

[*Received*: 22.1.2015; *accepted*: 3.2.2015]